Candidate HPV-Specific T-Cells Expand in the Tumor Microenvironment During Chemoradiotherapy

Lauren Colbert (LColbert@mdanderson.org)
The University of Texas MD Anderson Cancer Center
Molly El Alam
The University of Texas MD Anderson Cancer Center https://orcid.org/0000-0001-5717-7024
Erica Lynn
The University of Texas MD Anderson Cancer Center
Julianna Edwards
University of Texas MD Anderson Cancer Center
Tatiana Karpinets
The University of Texas MD Anderson Cancer Center
Xiaogang Wu
The University of Texas MD Anderson Cancer Center
Bhavana Chapman
The University of Texas MD Anderson Cancer Center
Travis Sims
The University of Texas MD Anderson Cancer Center https://orcid.org/0000-0003-1975-0795
Daniel Lin
The University of Texas MD Anderson Cancer Center
Ramez Kouzy
The University of Texas MD Anderson Cancer Center
Greyson Biegert
The University of Texas MD Anderson Cancer Center
Andrea Delgado Medrano
The University of Texas MD Anderson Cancer Center
Adilene Olvera
The University of Texas MD Anderson Cancer Center
K. Sastry
The University of Texas MD Anderson Cancer Center
Patricia Eifel
The University of Texas MD Anderson Cancer Center
Anuja Jhingran
The University of Texas MD Anderson Cancer Center
Lilie Lin

University of Texas MD Anderson Cancer Center https://orcid.org/0000-0001-7681-8966
Lois Ramondetta
The University of Texas MD Anderson Cancer Center
Andrew Futreal
The University of Texas MD Anderson Cancer Center https://orcid.org/0000-0001-8663-2671
Amir Jazaeri
University of Texas MD Anderson Cancer Center https://orcid.org/0000-0003-4335-4151
Kathleen Schmeler
The University of Texas MD Anderson Cancer Center
Jingyan Yue
McGovern Medical School at UTHealth
Aparna Mitra
The University of Texas MD Anderson Cancer Center
Kyoko Yoshida-Court
The University of Texas MD Anderson Cancer Center
Jennifer Wargo
MD Anderson https://orcid.org/0000-0003-3438-7576
Travis Solley
The University of Texas MD Anderson Cancer Center
Venkatesh Hegde
The University of Texas MD Anderson Cancer Center
Sita Nookala
The University of Texas MD Anderson Cancer Center
Ananta Yanamandra
The University of Texas MD Anderson Cancer Center
Stephanie Dorta-Estremera
University of Puerto Rico, Medical Sciences Campus
Geena Mathew
The University of Texas MD Anderson Cancer Center
Rohit Kavukuntla
The University of Texas MD Anderson Cancer Center
Cassidy Papso
The University of Texas MD Anderson Cancer Center
Mustapha Ahmed-Kaddar
The University of Texas MD Anderson Cancer Center
Minsoo Kim
The University of Texas MD Anderson Cancer Center
Jianhua Zhang
The University of Texas MD Anderson Cancer Center https://orcid.org/0000-0001-5412-9860

Alexandre Reuben
The University of Texas MD Anderson Cancer Center https://orcid.org/0000-0003-4510-0382
Emma Holliday
The University of Texas MD Anderson Cancer Center
Bruce Minsky
The University of Texas MD Anderson Cancer Center
Albert Koong
The University of Texas MD Anderson Cancer Center
Eugene Koay
The University of Texas MD Anderson Cancer Center https://orcid.org/0000-0001-7675-3461
Prajnan Das
The University of Texas MD Anderson Cancer Center
Cullen Taniguchi
The University of Texas MD Anderson Cancer Center https://orcid.org/0000-0002-8052-3316
Ann Klopp
The University of Texas MD Anderson Cancer Center

Article

Keywords: Human papillomavirus (HPV), tumor-specific antigens, chemoradiotherapy, T-cell assays

Posted Date: March 16th, 2021

DOI: https://doi.org/10.21203/rs.3.rs-105933/v1

Abstract

Human papillomavirus (HPV) infection causes 600,000 new cancers worldwide each year. HPV-related cancers express the oncogenic proteins E6 and E7, which could serve as tumor-specific antigens. It is not known whether immunity to E6 and E7 evolves during chemoradiotherapy (CRT) or affects survival. We used functional T-cell assays to identify candidate HPV-specific T-cells and T- cell motifs common across 86 patients with HPV-related cancers. These HPV-specific clones and E7-related motifs expanded over the course of treatment, whereas non-HPV-specific T-cells did not. In HPV16+ patients, improved recurrence-free survival was associated with this HPV-responsive T-cell expansion during CRT.

Introduction

Radiotherapy, a cornerstone of treatment for HPV-associated cancers, functions as an *in situ* vaccine, generating systemic antigen-specific immunity to tumor-specific antigens[1]. Chemoradiation therapy (CRT) can increase antitumor immunity in immunotherapy-resistant patients, such as those with disease progression on checkpoint inhibitor therapy[2,3]. Preclinical studies have demonstrated that radiation can enhance the diversity and abundance of the major histocompatibility type I (MHC-1) peptide repertoire, increase the presentation of cancer neoantigens to T-cells, promote the infiltration of lymphocytes into tumor, and augment the activation of cytotoxic T-cells[4–6]. However, these complex processes' clinical relevance in response to radiotherapy is unclear.

In this study, we used human papillomavirus (HPV)-associated cancers as a model for investigating antigen-specific immune response to chemoradiotherapy (CRT). HPV-associated cancers are unique in that they express the viral oncoproteins E6 and E7, which can serve as tumor-specific antigens[7,8]. HPV integration into the host's cellular genome results in stable E6 and E7 expression, which inhibits the function of p53 and retinoblastoma (Rb), leading to the transformation of the mucocutaneous epithelium into dysplastic and ultimately malignant cells[9]. HPV-associated squamous cell carcinomas are among the most exquisitely radiation-sensitive solid tumors[10] and in many cases can be eliminated with radiotherapy or CRT alone without surgical resection. Thus, HPV-associated squamous cell carcinomas are ideal models for studying the effect of CRT on antigen-specific immune response.

In the present study, we quantified antigen-specific immune activation during CRT by identifying and tracking candidate HPV-responsive T-cells in both the tumor microenvironment (TME) and peripheral blood in a large cohort of patients with a variety of HPV-related cancers. We used functional HPV antigen stimulation assays to identify these candidate HPV-specific and HPV-responsive T-cell clones, and then followed their presence and proportions over time in serially sampled tumor and blood from patients with HPV-related cervical, anal, vulvar, or vaginal cancers. We analyzed these clones' associations with survival. We also used multiparametric flow cytometry and T-cell receptor (TCR) sequencing to quantify immune subsets and analyzed these subsets' associations with survival after CRT.

Results

Identification of candidate HPV-specific clones. TCR sequencing data generates innumerable potential TCR sequences for each sample, any of which could be HPV-specific. Currently, public databases contain limited data on HPV-related sequences. Performing T-cell assays with peptide stimulation allows the identification of candidate clones that are HPV-reactive. We hypothesized that T-cell clones specific for HPV antigens could be identified based on ex vivo expansion following incubation with HPV peptides. To test this hypothesis, we performed functional T-cell assays using tumor brushings obtained from 2 patients with cervical cancer who had received 5 weeks of CRT. Tumor cytobrush specimens were collected to sample a mixed population, including lymphocytes and antigen-presenting cells, (APCs) from the TME. The mixed cell populations were cultured with peptides spanning the HPV16 E6 and E7 genes **(Supplemental Table 1)**; phorbol myristate acetate (PMA)/ionomycin cocktail to stimulate lymphocyte signaling and proliferation in a non-antigen-specific manner; or with untreated media (control). The HPV peptide cocktail was composed of 13 peptides (each comprising 25-35 amino acids) that span the HPV16 E6 and E7 proteins and are immunogenic in the HPV vaccine[11–16]. These long peptides are processed and presented by antigen-presenting cells to HPV-specific intratumoral lymphocytes. The mixed cell cultures and HPV peptides or controls were incubated overnight to allow the expansion of HPV-specific T-cells. DNA extracted from the mixed cell cultures was isolated and subjected to TCR sequencing of the CDR3B region (immunoSEQ, Adaptive Biotech). Unique clones were identified in each treatment condition; a minority of clones were identified in multiple samples **(Fig. 1a-c),** suggesting that the incubation conditions altered the subset of intratumoral clones that proliferated ex vivo. Seven potential categories of clones were identified; T-cell clones identified in HPV peptide-treated cultures ($HPV^+PMA^-CTRL^-$, n = 1,113; HPV^+PMA^+, n = 108; and HPV^+CTRL^+, n = 64) were considered "HPV-responsive," and T-cell clones identified in only the HPV^+ wells ($HPV^+PMA^-CTRL^-$; n = 1,113) were considered "HPV-specific." For clones present in both patients, clones with "contradicting" results (negative in 1 patient, positive in another) were not included in the pools of HPV-responsive or HPV-specific clones. Detailed annotations of the candidate HPV clones are listed in **Supplemental Table 2.** Annotations of HPV-related clones **(Supplemental Table 3)** in public TCR databases are extremely limited and thus were not utilized for this analysis.

Identification of candidate HPV-reactive clones in HPV-related cancers in patients undergoing CRT. This approach of using HPV peptide stimulation to identify HPV-reactive T-cells was initially validated in 1 patient by searching that patient's TCR sequencing data in serial tumor samples **(Fig. 1e, f)**. Notable distinct kinetics were observed for candidate HPV-specific clones as compared with the 100 most abundant clones overall. Candidate HPV-specific clones decreased and then expanded by week 5, whereas the relative frequency of the most abundant clones overall increased in week 1 and then declined in relative frequency by week 5.

Next, we sought to determine whether these candidate HPV-reactive clones were patient-specific or present in other patient samples. We performed TCR CDR3 ß-chain sequencing analysis of blood and tumor specimens collected from 86 patients with HPV-related cancers at 5 time points over the course of CRT (baseline; weeks 1, 3, and 5 of CRT; and 3 months after CRT [follow up]). All 86 patients had locally

advanced HPV-related cancers amenable to definitive CRT. Of these patients, 67 (78%) had cervical cancer, 13 (15%) had anal cancer, 4 (5%) had vaginal cancer, and 1 (1%) had vulvar cancer. Patient and tumor characteristics are summarized in **Table 1**, and samples collected at each time point are described in **Supplemental Table 4**. The overall study design is shown in **Fig. 1d.** Most patients had squamous cell carcinoma (84.9%), positive nodal status (69.8%), and stage II or III disease (38.4% and 33.7%, respectively), although staging systems differed among disease types. Viral strains identified in patients in whom HPV viral DNA was detected included HPV16 (60.5%) and HPV18 (21.1%), which is consistent with prior reports of HPV genotyping for HPV-related cancers[17–19].

Individual clones were present across multiple time points in a median of 9 patients (range, 0 – 35 patients for unique clones) and at any time point in a median of 12 patients (range, 0 – 65 patients). The most commonly identified clones are shown in **Fig. 1g**. The most commonly identified clone in tumors, CASSLGQGYEQYF, was identified in 30 tumor samples and 28 peripheral blood samples. The second most commonly identified clone in tumors, CASSLGGTEAFF, was identified more often in peripheral blood samples (n = 36) than in tumor samples (n = 26). These 2 clones were present at baseline in multiple patients in peripheral blood (n = 18) **(Supplemental Fig. 1a)** and tumor (n = 62) **(Supplemental Fig. 1b)**, but the overall proportions of these clones were quite low in both blood (maximum proportion = 0.0005) **(Supplemental Fig. 1c**) and tumor (maximum proportion = 0.006) **(Supplemental Fig. 1d)**.

HPV-specific T-cells expand in tumor, whereas non-specific T-cells contract in tumor and blood. Next, we reasoned that if the candidate HPV-reactive clones recognize HPV antigens, they may uniquely expand in the TME during CRT as a result of increased antigen presentation induced by CRT. Counts of HPV-responsive (HPV^+; either $PMA^{+/-}$ or $CTRL^{+/-}$) clones increased in blood by week 5 ($P < 0.05$) **(Fig. 2b)** and increased even more in tumor at each time point and by week 5. Non-specific PMA-responsive clones (PMA^+; either $HPV^{+/-}$ or $CTRL^{+/-}$) showed no change from baseline in either sample type **(Fig. 2a)**. Overall, T-cell clonality slightly increased in blood, but decreased in tumor, from baseline to week 5 **(Fig. 2c).** Only the most HPV-specific group ($HPV^+PMA^-CTRL^-$), changed differently in tumor versus blood, which might explain this difference. Changes over time for all groups are presented in **Supplemental Table 5**. Non-specific T-cell counts decreased in both blood and tumor from baseline to week 5 ($P = 0.02$ and $P < 0.01$, respectively) **(Fig. 2d)**. Although HPV-specific T-cell counts also decreased in blood (6 vs. 1; $P < 0.01$), they expanded in tumor (0 vs. 2; $P < 0.01$) **(Fig. 2e)**. The median proportions of HPV-specific clones in tumor were 0.025% at baseline and 0.044% at week 5, whereas the median proportions of HPV-specific clones in blood were 0.05% at baseline and 0.034% at week 5. Subset analyses of all HPV^+ patients and only $HPV16^+$ patients showed that by week 5, HPV^+ clones increased significantly in tumor (HPV^+ subset: 0 vs. 0.00004, $P = 0.002$; HPV16 subset: 0 vs. 0.000023, $P = 0.01$) but were unchanged in blood (HPV^+ subset: $P = 0.42$; HPV16 subset: $P = 0.5$).

Identification of and changes in E7-specific TCR motifs during CRT. Using the Grouping of Lymphocyte Interactions by Paratope Hotspots (GLIPH) clustering algorithm[20], we identified 5 amino acid motifs in HPV antigen-stimulated T-cell populations (minimum $P = 0.001$) **(Fig. 3)**. Although we used immunoSEQ

TCR sequencing to sequence the β chain of the CDR3 complex, the TCR complex actually contains both α and β chains as well as the signaling molecules CDδ, CD3γ, CD3ε, and CD3ζ. GLIPH is a computational algorithm that predicts significant motif lists and convergence lists of motifs based on individual TCR sequences, including known HLA type when available. The software provides enrichment for each motif, V-gene, CDR3 length, and proliferation counts.

Of these 5 motifs (QSRANV, KTYG, GTRF, PIW, and RHH) **(Fig. 3a-e)**, 3 (QSRANV, KTYG, and GTRF) were not found in control conditions but were enriched in response to HPV peptides and, to a lesser degree, in response to PMA (QSRANV, 13/4284 template clones [0.30%] for HPV peptides vs. 6/7294 clones [0.08%] for PMA; KTYG, 6/4284 clones [0.14%] vs. 4/7294 clones [0.05%]; GTRF, 4/4284 clones (0.09%] vs. 1/7294 clones [0.01%]).

The 2 most differentially enriched motifs, QSRANV and KTYG, were also the most common in our patient population, identified in 40% and 33% of patients (p<.01), respectively, as compared with 13% for PIW, 9% for GTFR, and 7% for RHH **(Supplemental Table 6)**. The QSRANV motif had higher proportions than all but the KTYG motif ($P < 0.01$). These motifs were also more likely to proportionally increase throughout CRT (each increased in patients) **(Fig. 3f,i)**. Proportion of the QSRANV motif increased significantly more than all other motifs ($P < 0.01$ for all). Conversely, 12 of 17 patients with the PIW motif had decreases in the motif proportion in the TME **(Fig. 3g)**, whereas only about 50% of patients with the GTFR and RHH motifs at baseline had an increase over time **(Fig. 3h,j)**.

When the CDR3β receptor sequences for these enriched motifs were cross-referenced to known pathogenic TCR sequences using the McPAS-TCR database[21] epitopes to both QSRANV and KTYG mapped to a conserved region of an essential viral oncogenic domain that disables the Rb tumor suppressor. This same domain is necessary for the association of the HPV oncoprotein E7 with the Rb tumor suppressor protein and is a key mediator in the oncogenic transformation of HPV-related cancers[22], validating the finding that these motifs are likely E7-related.

The association of HPV-responsive T-cell expansion with survival outcomes is limited to HPV16$^+$ patients. To determine whether this HPV-specific expansion within the TME was associated with survival, we performed univariate Cox proportional hazard modeling for recurrence-free survival (RFS) and overall survival (OS) with *P*-value correction for multiple testing. We found no significant relationship between survival and the count, proportion, or presence of HPV-specific or HPV-responsive clones at any time point **(Supplemental Table 7)**. Fold changes in HPV-specific or HPV-responsive clone populations in the TME or blood from baseline to week 5 also were not clearly associated with RFS or OS. Whereas fold change in HPV-responsive clones in the TME was not associated with RFS in all patients (hazard ratio [HR] 0.75 [95% confidence interval (CI) 0.53-1.07]; $P = 0.11$), this change was significantly associated with RFS in only HPV16+ patients (HR 0.38 [95% CI 0.15-0.93]; $P = .04$) **(Supplemental Fig. 2)**, suggesting that any survival benefit is limited by the HPV subtype.

The static counts, proportions, and fold changes over time of E7-related motifs were not significantly associated with RFS or OS **(Supplemental Table 8)**. Higher fold changes in only 1 motif, PIW, from baseline to week 5 were significantly associated with improved RFS (HR 1.04 [95% CI 1.01-1.07]; *P* = 0.007) but not OS (*P* = 0.14). The PIW motif, which was enriched in HPV-stimulated populations as compared with control populations (0.09% vs. 0.03%) but not present in PMA-stimulated populations, may represent an HPV-specific but non-reactive motif. Repeating this analysis for subsets of HPV^+ and $HPV16^+$ patients yielded consistent findings.

Immune phenotypes associated with HPV-specific expansion. We also profiled the intratumoral and peripheral immune milieu during CRT to identify changes associated with HPV-specific T-cell remodeling. Multiparametric flow cytometry was used to assess samples from 86 patients after stimulation with either HPV peptides or media (control). Markers included those of lymphocyte and myeloid lineages, including functional markers of activation (CD69, IFNγ, granzyme B [Grzb], Ki67) and exhaustion (CTLA4, PD-1). HPV antigen-specific T-cells were analyzed with intracellular staining for IFN-producing $CD8^+$ T-cells following stimulation with overlapping peptides spanning the E6 and E7 genes from HPV16.

Overall, the most substantial changes in the TME immune cell composition were significantly increased percentages of $PD1^+CD8^+$ and $PD1^+CD4^+$ T-cells at follow-up as compared with baseline (*P* = 0.01 and *P* = 0.03, respectively) **(Supplemental Fig. 3 and 4 and Supplemental Table 5)**. The expression levels of markers of early clonal priming and activation (PD-1, CD69, IFN, and Grzb) increased during CRT and peaked at either week 3 (PD-1) or at the end of treatment (CD69, IFN, and Grzb) and were sustained in the treated tumor at week 12 **(Supplemental Fig. 3l and Supplemental Table 5)**.

In peripheral blood, the percentage of $CD8^+$ T-cells with the activation markers CTLA-4 and Ki67 increased during CRT (week 3 for CTLA-4, *P* = 0.03; week 3 and week 5 for Ki67, *P* = 0.04 and *P* = 0.04, respectively) as compared to baseline **(Supplemental Fig. 3 and Supplemental Table 5)**. There was no significant change in HPV peptide-responsive IFN^+CD8^+ expression in blood or TME between the start of treatment and week 5**.** Testing for differences in the fold changes of certain markers between blood and tumor showed that productive clonality of T-cell repertoires increased in blood and decreased in tumor samples at week 3 (blood: 0.08, tumor: -0.97; *P*=0.008) and week 5 (blood: 0.04, tumor: -0.53; *P*=0.009) (**Supplemental table 9)**.

Peptide-specific activation, measured by IFN^+CD8^+ expression, was not associated with any clinical variables (age, body mass index, nodal status, disease stage, or tumor histology) in either blood or tumor **(Supplemental Table 10 and Supplemental Table 11)**. Higher overall $CD8^+$ counts were associated with lower BMI (*P* < 0.01) and negative nodal status (*P* < 0.01). Higher non-specific (media responsive) IFN^+CD8^+ expression in blood was associated with younger age (*P* < 0.01).

To better describe the immune phenotypes associated with HPV-reactive clone remodeling, we used model-based clustering using the mclust package[23] for Gaussian mixture modeling for peptide-responsive $CD4^+$ and $CD8^+$ markers **(Fig. 4a)**. Clustering revealed several distinct clusters distinguished

primarily by these same markers of early priming (PD1) and activation (Grzb, IFN, Ki67) **(Fig. 4b)**. One cluster, which was characterized by a rich population of PD-1$^+$CD4$^+$ and PD-1$^+$CD8$^+$ subsets, was seen in patients with high HPV-specific remodeling at baseline **(Fig. 4c)** but disappeared at week 1. By week 5, these patients demonstrated CD8$^+$ activation (Ki67$^+$CD8$^+$ cells, CD69$^+$CD8$^+$ cells), suggesting an "early priming/activation" pattern.

We also performed unsupervised hierarchical clustering with all clinical variables **(Supplemental Fig. 5).** Non-squamous cancers were enriched over squamous cancers in immune poor cluster membership vs. early priming/activation cluster membership (P = 0.02), with a similar profile at all time points rather than a change over time. For patients with HPV remodeling, defined as a fold change >1.5 in HPV-specific clones in the TME from baseline to week 5, the immune phenotype shifted over time from overall activation at baseline (high CD8$^+$ T-cells, high CD4$^+$ T-cells, low T-regulatory cells [Tregs]) to immune exhaustion at week 1 and then to activation and memory markers at week 5 (CD8$^+$Grzb$^+$, CD8$^+$CD69$^+$). Patients with HPV remodeling also exhibited an overall shift from CD8$^+$ activation to CD4$^+$ memory markers.

Immune phenotypes associated with survival. On univariate analysis, higher populations of Tregs (FOXP3$^+$CD4$^+$ cells) in peripheral blood at baseline were associated with lower RFS (HR 1.13 [95% CI 0.03-0.22]; P = 0.01) and OS (HR 1.12 [95% CI 1.02-0.21]; P = 0.02). Higher populations of exhausted T-cells (CTLA4$^+$CD4$^+$ cells) in blood samples at baseline were also associated with poorer RFS (HR 1.29 [95% CI 0.03-0.48]; P = 0.027) and OS (HR 1.31 [95% CI 1.05-0.5]; P = 0.02) **(Supplemental Table 7)**. Higher populations of activated T-cells (IFN$^+$CD8$^+$ cells) in peripheral blood at the end of treatment (week 5) were associated with improved RFS (HR 2.12 [95% CI 1.08-4.53]; P = 0.03) and OS (HR 2.49 [95% CI 1.17-5.31]; P = 0.02). Sensitivity analyses by tumor type (anal, cervical, vaginal, and vulvar) and histology (squamous cell carcinoma vs. all others) showed no differences from the full-set analysis. Subset analyses of HPV$^+$ patients and HPV16$^+$ patients were also performed. For HPV$^+$ patients, higher proportions of intratumoral Ki67$^+$CD8$^+$ cells at baseline were associated with improved RFS (P = 0.009) and OS (P = 0.048). For HPV16$^+$ patients, there were no significant associations between flow parameters and survival.

Discussion

The findings of our study inform the development and testing of immune-based therapies for HPV-related cancers, especially in the up-front or definitive setting and in combination with standard-of-care CRT. Radiotherapy affects the equilibrium of the immune system by increasing proportions of Tregs, decreasing proportions of functional, activated cytotoxic T-cells, and increasing dendritic cells' presentation of tumor antigens. Our data findings suggest that although radiation may lead to antigen-specific T-cell activation increases in response to HPV antigens. Assuming that HPV antigens could serve as surrogates for antigen-specific tumor response in HPV-related cancers, we used functional T-cell assays to identify candidate HPV-specific T-cell sequences, confirmed that these T-cell sequences were

present across several patients with HPV-related cancers, and discovered that these HPV-specific T-cells increase in the TME during CRT. In HPV16$^+$ patients, these T-cells were associated with RFS.

The HPV-specific T-cell population we identified within the TME could be a surrogate for tumor antigen-specific immune response across cancer types. Although radiation can directly cause T-cell apoptosis, it can also upregulate MHC-1 expression, thereby increasing antigen presentation and activated T-cell expansion, which is particularly useful if this response is a tumor antigen-specific response. In addition, the activation or stimulation of interferon genes through cytosolic DNA pathways induced by radiation also results in the infiltration of T-cells into the tumor[6]. Thus, the addition of radiotherapy in patients receiving immunotherapy for progressive disease could spur the release tumor antigens to function as a vaccine to achieve an antigen-specific immune response and reignite immune responses[1].

Further, combining radiotherapy with immunotherapies targeting the HPV-specific T-cell population may improve outcomes. The T-cell populations and motifs we identified were not strongly associated with outcomes, which suggests that T-cell response alone is not sufficient complete tumor response. Patients in whom HPV remodeling did not occur demonstrated low CD8$^+$ activation throughout treatment, suggesting that these patients lack a priming response and may not benefit as much from immune checkpoint therapy in combination with CRT. Although higher populations of activated cytotoxic T-cells in peripheral blood at the end of treatment were associated with improved RFS and OS, higher populations of Tregs and exhausted T-cells at baseline were associated with lower RFS and OS. This suggests that anti-Treg therapy or anti-CTLA4 therapy can facilitate radiation's stimulation of the antigen-specific immune response. Clustering analysis revealed that patients with high HPV-specific remodeling had one cluster characterized by a rich population of PD-1$^+$CD4$^+$ and PD-1$^+$CD8$^+$ subsets at baseline. By week 5, these patients demonstrated CD8$^+$ activation (Ki67$^+$CD8$^+$ cells, CD69$^+$CD8$^+$ cells), suggesting an "early priming/activation" pattern; therefore, this cluster may represent patients in whom the early addition of checkpoint inhibitor therapy might improve immune response. The fact that immune profiles changed over time for squamous cancers, but not non-squamous cancers suggests that the immune microenvironment of squamous cancers is more susceptible than that of non-squamous cancers to this remodeling by CRT and helps explain the increased radiosensitivity of some squamous cancers.

Little is known about the intratumoral T-cell repertoire of HPV-related cancers. Cui et al.[24], using TCR sequencing to characterize the peripheral T-cell repertoires of 25 patients with cervical cancer or cervical dysplasia and those of healthy patients, found that differences in spatial heterogeneity and diversity were associated with cervical cancer; however, the samples in that study were primarily peripheral blood samples, and sequencing was performed at only 1 time point. We also identified several of the T-cell clones Cui et al.[24] identified, as well as motifs found to be associated with Rb in other previous studies, but we also identified potentially novel sequences and motifs. Still, the known E7 clustering motifs were the most frequent in our patient population, and for nearly every patient in the present study, these E7-related motifs were increased at the end of CRT. Changes in the known E7-related motifs were not associated with survival; however, one of the unknown motifs, PIW, was associated with RFS but was less

common among our patients. PIW may be an HPV-related motif that, owing to its infrequency, may be associated with survival in a larger cohort, or it may be a non-functional HPV-responsive motif. Further study of these motifs in a larger population of patients with a specific HPV subtype is warranted.

One limitation of the present study was its lack of an evaluation of the functional capacity of the HPV-specific T-cells. Although we performed HPV antigen stimulation and flow cytometry, this approach is less sensitive than functional T-cell assays with TCR sequencing for detecting antigen-responsive T-cells[25]. Although these T-cells are present and expanded at baseline, they could be dysfunctional or exhausted after CRT. Future studies should undertake long-term tracking of T-cells in patients undergoing CRT and should provide further phenotyping of these HPV-specific T-cells to drive engineered immunotherapy approaches.

Online Methods

Participants and clinical data. Patients with biopsy-confirmed locally advanced cervical, vaginal, vulvar, and anal cancers were enrolled in an IRB-approved (2014-0543) multi-institutional prospective clinical trial at The University of Texas MD Anderson Cancer Center and the Harris Health System Lyndon B. Johnson Hospital Oncology Clinic from September 22, 2015, to January 11, 2019. Cases of cervical and anal cancer were staged according to the FIGO 2009 staging system and the AJCC 7th edition staging system, respectively, which were in place when the study began. Patients were required to have a visible tumor and planned standard-of-care treatment for intact cancer. For cervical cancer, this involved definitive radiotherapy, including external beam radiotherapy and brachytherapy, with concurrent cisplatin. Patients with anal cancer received external beam radiotherapy with concurrent cisplatin and 5-fluorouracil. Patients with vaginal cancer received external beam radiotherapy and concurrent cisplatin with or without brachytherapy. Patients with vulvar cancer received concurrent cisplatin without brachytherapy. Patients with any previous pelvic radiotherapy were excluded. Patients receiving external beam radiotherapy received a minimum radiation dose of 45 Gy in 25 fractions over 5 weeks. Clinical, demographic, and pathologic data were collected prospectively.

Sample collection, DNA extraction, and TCR sequencing. Radiation oncology or gynecologic oncology clinicians at either MD Anderson Cancer Center or Lyndon B. Johnson Hospital used Isohelix buccal swabs (Isohelix, cat. #DSK-50) to collect tumor DNA samples. Patients underwent swabbing 5 times: at baseline, at the end of week 1 (after 5 fractions), at the end of week 3 (after 10-15 fractions), within 1 week before the first brachytherapy treatment or at the time of brachytherapy (week 5), and at the first follow-up visit (typically 12 weeks after treatment). For each patient, all samples were obtained from the same general tumor region. Peripheral serum samples were also collected at baseline, week 1, week 3, week 5, and follow-up. DNA was extracted from the tumor swab samples with the Isohelix Xtreme DNA lysis kit per the manufacturer's instructions (Isohelix, cat. #XME-50). DNA was extracted from blood samples after Ficoll gradient separation with the DNeasy Blood and Tissue Kit (Qiagen, cat. #69504) according to the manufacturer's instructions and without modification for erythrocytes. At these same

timepoints, cytobrush samples of the patients' tumors were also collected as described previously[12] and used for flow cytometry.

Blood samples were collected in 10-mL ethylenediaminetetraacetic acid (EDTA)-containing tubes (BD Biosciences, cat. #366643) and diluted with 1 ´ phosphate-buffered saline (PBS) at a 1:1 ratio by volume. The diluted blood was then distributed into 50-mL conical tubes containing 8-mL aliquots of Ficoll-Paque PLUS Media (GE Healthcare, cat. #17144002). Each sample was spun at 400 x *g* with the brake off for 40 minutes at room temperature. The peripheral blood mononuclear cell layer was then removed using a serological pipette and placed into a Falcon 50-ml conical centrifuge tube. Twenty-five milliliters of 1 x PBS was added, and the sample was centrifuged at 400 x *g* for 10 minutes. The supernatant was discarded, and the pellet was resuspended in 10 mL of RPMI 1640. The cells were washed once more by centrifuging the sample at 400 x *g* for 10 minutes, disposing the supernatant, and then resuspending the cells in 10 ml of RPMI 1640. The cells were then counted and separated into aliquots of approximately 5 x 10^6 cells each. The aliquots were centrifuged again at 400 x *g* for 10 minutes at room temperature, the supernatant was removed, and the dry pellets were frozen in cryovials.

To Isolate DNA from peripheral blood mononuclear cells for TCR sequencing, the DNeasy Blood and Tissue Kit (Qiagen, cat. #69504) was used following the manufacturer's instructions without modification for erythrocytes. Proteinase K (20 µl) and 5-10 µl of the frozen pellet were added to a 2-ml microcentrifuge tube and PBS was added to bring the total volume to 220 µl. Ethanol-free Buffer AL (200 µl) was added to the tube, which was vortexed to mix and homogenize the sample, which was then incubated at 56°C for 10 min. Following incubation, 200 µl of ethanol was added to the sample and mixed thoroughly via vortex. The entire mixture was then placed into a spin column in a 2-ml collection tube. The tube was centrifuged at 6000 x *g* for 1 minute at room temperature, and the collected liquid was discarded. The spin column was transferred into a new 2-ml collection tube, 500 µl of Buffer AW1 was added, and the column was centrifuged for 1 minute at 6000 x *g* at room temperature; the collected liquid and tube were discarded. The spin column was transferred into a new collection tube, 500 µl of Buffer AW2 was added, and the tube was centrifuged for 3 minutes at 20,000 x *g* at room temperature to completely dry the column's membrane. The collected liquid and 2-ml collection tube were discarded. The dried column was placed into a 2-ml microcentrifuge tube, and 200 µl of Buffer AE was added to the membrane, which was incubated at room temperature for 1 minute. The tube was centrifuged for 1 minute at 6000 x *g* at room temperature. The resultant DNA elution was then used for TCR sequencing.

Multiplex PCR-based deep sequencing of the CDR3 region of TCRβ was performed using the proprietary immunoSEQ immune profiling system (Adaptive Biotechnologies). This system uses a library of known forward primers, each specific to a TCR Vβ segment, and reverse primers specific to a TCR Jβ segment. Both productive templates and nonproductive templates (CDR3 regions predicting out-of-frame receptor genes or premature stops) were assessed, but only the productive templates were included in the final analysis.

HPV Genotyping. Tumor swab DNA isolates were applied to the Linear Array HPV Genotyping Test and Linear Array Detection Kit (Roche, cat. #04472209 190 and #03378012 190, respectively).

The Working Master Mix was prepared by adding 125 mL of HPV Mg^{2+} to one vial of HPV MMX and mixing by inversion 10-15 times. Then, 50 mL of Working Master Mix was combined with 50 mL of isolated DNA in each reaction tube. Amplification was performed in an Applied Biosystems Gold-plated 96-Well GeneAmp PCR System 9700 with the following program: HOLD 2 min at 50°C; HOLD 9 min at 95°C; CYCLE (40 cycles, ramp rate 50%) 30 sec at 95°C, 1 min at 55°C, 1 min at 72°C; HOLD 5 min at 72°C; HOLD 72°C Indefinitely. Less than 4 hours after amplification, 100 mL of Denaturation Solution (DN) was added to the amplification products and mixed by pipetting.

For the hybridization reaction, HPV Strips containing probes were placed in wells of a 24-well tray (Roche, cat. #03140725 001). Working Hybridization Buffer (100 mL SSPE, 12.5 mL SDS, and 388 mL deionized water) and 75 mL of denatured amplicon was added to each well. The tray was hybridized in a shaking water bath at 53°C for 30 min with a shaking speed of 60 RPM. For this step and for each following step, each buffer was removed from the strips by vacuum aspiration. The strips were washed first with 4 mL Working Ambient Wash Buffer (133 mL SSPE, 13.3 mL SDS, and 2520 mL deionized water) by rocking plate 3-4 times, and then with 4 mL Working Stringent Wash Buffer in the shaking water bath at 53°C for 15 min with a shaking speed of 60 RPM.

To begin the detection process 4 mL of the Working Conjugate was added to each well and incubated for 30 min at room temperature on an orbital shaker at 60 RPM. To wash the conjugate off the strips, three rinses were performed by adding 4 mL Working Ambient Wash Buffer. In the first of these rinses, the tray was rocked gently 3-4 times, but for the second and third rinses the tray was shaken at 60 RPM on an orbital shaker at room temperature for 10 min. Then, 4 mL of Working Citrate Buffer (25 mL CIT and 475 mL deionized water) was applied to each well and the tray was shaken at 60 RPM on an orbital shaker at room temperature for 5 min. After removing the final buffer by vacuum filtration, 4 mL of Working Substrate (4 mL SUB A and 1 mL SUB B) was added to the wells and the tray was shaken at 60 RPM on an orbital shaker at room temperature for 5 min. The substrate was aspirated from the wells and a final rinse of 4 mL deionized water was applied to each well containing a strip.

Each strip was removed from the tray by forceps and dried on a clean surface for an hour. Results were interpreted by aligning each strip with the Linear Array HPV Genotyping Reference Guide. HPV genotypes corresponding with positive bands on the strips were recorded for each sample. The results were validated by confirming that the negative control showed no bands, the positive control showed bands for HPV16, and the b-globin internal controls were present on each sample strip and the positive control strip.

Flow cytometry. Cells were dislodged from cytobrush samples using vortex agitation. Dithiothreitol solution (1X Hank's balanced salt solution, 4% bovine serum albumin, 2 mM dithiothreitol; Invitrogen, cat. #P2325) was added for mucous breakdown if large amounts of mucous were present, and cells were passed through a 70-um cell strainer. After centrifugation, cell pellets were suspended in sterile complete

RPMI media containing penicillin-streptomycin and gentamicin antibiotics (Fisher Scientific, cat. #SH30027FS, #SV30010, and #BW17-518Z, respectively).

Lymphocytes were isolated from peripheral serum samples by density gradient centrifugation with Lymphoprep medium (Fisher Scientific, cat. #NC0460539). The mononuclear cell layer was collected and resuspended in RPMI media.

Custom peptide sequences of 10 E6 and 4 E7 domains were commercially synthesized (Biosynthesis Inc). Cervical brush-derived cells were incubated with 10 ug/mL of pooled peptide at 37°C overnight (12-16 h). The next day, Golgiplug (BD Biosciences, cat. #555029) was added to the solution, and the solution was incubated at 37°C for 4-6 h to allow for IFN to accumulate. As a positive control for immune cell activation and cytokine production, following overnight incubation in media alone, cells were incubated with cell activation cocktail containing PMA/ionomycin (BioLegend, cat. #423301/2) and Golgiplug at 37°C for 4-6 h prior to staining.

Lymphocyte immunostaining was performed according to standard protocols. Briefly, cells were fixed using the FOXP3/Transcription Factor Staining Buffer Set (eBioscience, cat. #00-5523-00) and stained with a 16-color panel of antibodies from BioLegend, BD Bioscience, eBioscience, and Life Technologies. Cells were stained with intracellular monoclonal antibody for 30 minutes at 4°C in the presence of anti-Cd16/Cd32 monoclonal antibody (BD Bioscience), fixed with FOXP3/Transcription Factor Staining Buffer Set (eBioscience, cat. #00-5523-00), and held in flow cytometry staining buffer (2 mM EDTA, 2% fetal bovine serum; Corning). Counting beads (Thermo Fisher) were used for single-color controls. The cells were analyzed using a 5-laser, 18-color LSRFortessa X-20 Flow Cytometer (BD Biosciences) and FlowJo 10.6.1.

Functional expansion of antigen-specific intratumoral T-cells. Cytobrush samples were collected as described previously[26]. Each sample was placed in a 15-ml conical tube and immediately transported to the lab, where 5 ml of cold RPMI-1640 with 10% fetal bovine serum and 1% penicillin/streptomycin were added to the tube. The tubes were vortex-agitated to dislodge cells into the media. For brushes with substantial mucus, 2 mm of dithiothreitol (Sigma) in Hanks' balanced salt solution (Invitrogen) with 4% bovine serum albumin (Sigma) was added and allowed to rest for 10 min at room temperature, after which cells were passed through a 70-um cell strainer. The samples were centrifuged for 5 minutes at 400 x *g* at room temperature and then washed twice by centrifuging and resuspending them in 10 mL of room-temperature RPMI media. After the second wash, cells were counted and resuspended so a minimum of 1.0 x 10^6 cells per 100 µl of solution could be placed in each well. One hundred microliters of solution were distributed into each of 3 wells on a 96-well round bottom plate. Each well contained 100 µl of a custom mix of HPV13-SLP peptide (10 ug/mL) **(Supplemental Table 1)**[11–16], 100 µl of PMA (50 ng/ml)/ionomycin (250 ng/ml) cocktail, or 100 µl of RPMI. The cells were cultured in an incubator at 37°C overnight (16-20 h). At that time 0.4 µL of Golgiplug at a 1:500 concentration was added to the wells and the plates incubated for another 4 to 6 h. The plate was centrifuged and the media aspirated, and the

cells were reconstituted with 200 µl of room-temperature 1x PBS and transferred into two 1.5-ml microcentrifuge tubes for DNA isolation.

DNA isolation was performed using the QIAamp UCP DNA Micro Kit (Qiagen, cat. #56204) according to the manufacturer's instructions.

All centrifugation steps were performed at room temperature, and samples and buffers were brought to room temperature prior to centrifugation. Proteinase K (10 µl) was added to the microcentrifuge tubes containing 100 µl of media. Then, 100 µl of Buffer AUL was added, and the samples were pulse-vortexed for 15 seconds and incubated at 56°C for 35 minutes. Samples were centrifuged at 17,800 x *g* for 3 minutes, and then 50 µl of ethanol was added. The samples were then pulse-vortexed and then incubated for 3 minutes at room temperature. The samples were centrifuged at 13,500 rpm 17,800 x *g* spin for 3 minutes and then transferred to the QIAamp UCP MinElute columns in 2-ml collection tubes and centrifuged at 13,500 rpm 17,800 x *g* for 5 minutes. Each column was transferred into a second collection tube and spun once more before being placed in another clean column. Buffer AUW1 (500 µl) was added to the column, which was centrifuged once more and then transferred to a clean collection tube. Buffer AUW2 (500 µl) was added to the column, which was again centrifuged and placed in a clean collection tube before being centrifuged once more at 17,800 x *g* for 5 minutes. The column was placed into a clean 1.5-ml centrifuge tube, and 100 µl of microbial DNA-free water was added to the column, which was incubated for 10 minutes at room temperature before being centrifuged at 17,800 x *g* for 5 minutes. Buffer AUE (100 µl) was added to the membrane, which was incubated for 10 minutes and centrifuged for 5 minutes. Next, 50 µl of Buffer AUE was added to the membrane, which was incubated for 10 minutes and then centrifuged for 5 minutes. Extracted DNA was then stored at 4°C until use. Isolated DNA was subjected to TCR sequencing (described above).

Analysis of flow and T-cell repertoire characteristics. The TCR metrics we studied were Total Templates, Productive Templates, Total Rearrangements, Productive Rearrangements, Productive Clonality, Sample Clonality, Productive Entropy, Max Productive Frequency, Max Frequency, and Out of Frame Rearrangements. To study changes in the flow characteristics over time, we compared the means for blood and tumor samples at each time point with baseline means by using a paired sample t-test. We compared median changes from baseline for TCR characteristics by using a Wilcoxon signed-rank test. We calculated the log2 fold change of any variable in blood or tumor samples that significantly changed from baseline. We then performed a Wilcoxon signed-rank test to assess if the degree of change differed between the blood and tumor samples. We also fit univariate Cox proportional hazards models for each of the flow and TCR variables at the static timepoints as well as for the fold changes in blood and tumor samples. Clustering of immune variables with and without clinical characteristics was performed using both machine learning algorithm "mclust" and using unsupervised hierarchical clustering. HPV remodeling was defined as a >1.5fold change in proportions of HPV-responsive clones.

Identification and analysis of HPV-specific clones. Public and exclusive repertoires were created for HPV peptide, PMA, and controls based on amino acid overlap in CDR3 sequences. Each sequence was

annotated using the mcPAS[21], VDJdb[27], and TBAdb[28] databases, downloaded on March 24, 2020. We then used the R package immunarch[29] to monitor the frequency of these HPV-specific CDR3 amino acid sequences over time as well as the most abundant clones overall. We also calculated the numbers of unique samples and patients that had each HPV-specific clone. To study whether the HPV-specific repertoire changes over time, we grouped clones from 2 patients based on the clones' presence in HPV, PMA, and control wells into 7 groups: $HPV^+PMA^+CTRL^+$, $HPV^+PMA^+CTRL^-$, $HPV^+PMA^-CTRL^+$, $HPV^+PMA^-CTRL^-$, $HPV^-PMA^-CTRL^+$, $HPV^-PMA^+CTRL^-$, and $HPV^-PMA^+CTRL^+$. We calculated the number and proportion of clones present in each sample and determined the clones' presence in each sample as a binary variable. We then compared the number and proportions of clones in blood and tumor samples for all 7 groups at each timepoint to those at baseline by using the Wilcoxon signed-rank test. We calculated the log2 fold change from baseline to determine if the degree of change is associated with survival. We also assessed whether the number and proportion of clones in these groups' blood and tumor samples were associated with survival by using a univariate Cox proportional hazards model.

We also performed the full analysis using subsets of data stratified by cancer type (anal vs. cervical, vaginal, and vulvar) and histology (squamous cell carcinoma vs. adenocarcinoma and adenosquamous carcinoma) and by HPV^+ and $HPV16^+$ subsets.

TCR motif identification and analysis. Significant motifs in the CDR3β portion of patient T-cell sequences relative to expected frequencies in a reference set of unselected naïve TCRs were identified using the (GLIPH) algorithm[20]. A local convergence minimum probability score cutoff of 0.001 and local convergent minimum observed versus expected fold-change of 10 was used. A simulated resampling depth of 1,000 was used. A minimum motif length of 3 was set, and discontinuous motifs were not allowed.

We built univariate Cox proportional hazard models for the counts and proportions of each motif at static time points as well as for the dynamic changes in the motifs from baseline. We also tested for baseline differences in the counts and proportions of the motifs using an analysis of variance test and conducted post hoc comparisons with a Bonferroni adjustment to identify differences between motifs. We also compared the proportions of motif absence or presence at baseline for each patient and assessed whether each patient experienced an increase or decrease in the proportion of each motif by week 5 using individual Fisher exact tests. We calculated the overall *P*-value for comparing all the motifs. The significance was adjusted for the 10 comparisons by dividing the type I error of 0.05 by 10. We tested for associations between clinical characteristics and $CD8^+$ (% Live Lymphocytes), CD4+ (% Live Lymphocytes), dendritic cells, and TCR characteristics in tumor and blood samples. Age and BMI were each fitted in a simple linear regression model. We used a Wilcoxon signed rank test to test for associations for nodal status, stage, and histology. Statistical significance was set at an α of 5% for a 2-sided *P*-value. All available samples were used for analyses. Analyses were conducted using RStudio 1.2.5033 Orange Blossom[30].

Declarations

This study was approved under the MD Anderson Cancer Center Institutional Review Board.

Acknowledgments

Supported in part by Cancer Center Support (Core) Grant P30 CA016672 from the National Cancer Institute, National Institutes of Health, to The University of Texas MD Anderson Cancer Center, The American Society for Clinical Oncology (ASCO) Young Investigator Award, and the MDACC HPV Moonshot. We also acknowledge assistance from the Department of Scientific Publications, including Joseph Munch and Chris Wogan.

Author Contributions

Lauren E. Colbert was involved in the study design, data acquisition, analysis and interpretation, and has drafted and approved the submitted version of the manuscript. She has agreed both to be personally accountable for her contributions and to ensure that questions related to the accuracy or integrity of any part of the work are appropriately investigated and resolved.

Molly B. El Alam was involved in the data acquisition, analysis and interpretation, and has drafted and approved the submitted version of the manuscript. She has agreed both to be personally accountable for her contributions and to ensure that questions related to the accuracy or integrity of any part of the work are appropriately investigated and resolved.

Erica J. Lynn was involved in the data acquisition, analysis and interpretation, and has drafted and approved the submitted version of the manuscript. She has agreed both to be personally accountable for her contributions and to ensure that questions related to the accuracy or integrity of any part of the work are appropriately investigated and resolved.

Julianna Bronk was involved in the data analysis and interpretation and has drafted and approved the submitted version of the manuscript. She has agreed both to be personally accountable for her contributions and to ensure that questions related to the accuracy or integrity of any part of the work are appropriately investigated and resolved.

Tatiana V. Karpinets was involved in the study design, data acquisition, analysis and interpretation, and has drafted and approved the submitted version of the manuscript. She has agreed both to be personally accountable for her contributions and to ensure that questions related to the accuracy or integrity of any part of the work are appropriately investigated and resolved.

Xiaogang Wu was involved in the data acquisition, analysis and interpretation, and has approved the submitted version of the manuscript. He has agreed both to be personally accountable for his contributions and to ensure that questions related to the accuracy or integrity of any part of the work are appropriately investigated and resolved.

Bhavana V. Chapman was involved in the data acquisition and has approved the submitted version of the manuscript. She has agreed both to be personally accountable for her contributions and to ensure that questions related to the accuracy or integrity of any part of the work are appropriately investigated and resolved.

Travis T. Sims was involved in the data acquisition, analysis and interpretation, and has approved the submitted version of the manuscript. He has agreed both to be personally accountable for his contributions and to ensure that questions related to the accuracy or integrity of any part of the work are appropriately investigated and resolved.

Daniel Lin was involved in the data acquisition and has approved the submitted version of the manuscript. He has agreed both to be personally accountable for his contributions and to ensure that questions related to the accuracy or integrity of any part of the work are appropriately investigated and resolved.

Ramez Kouzy was involved in the data acquisition and has approved the submitted version of the manuscript. He has agreed both to be personally accountable for his contributions and to ensure that questions related to the accuracy or integrity of any part of the work are appropriately investigated and resolved.

Greyson Biegert was involved in the data acquisition and analysis and has approved the submitted version of the manuscript. He has agreed both to be personally accountable for his contributions and to ensure that questions related to the accuracy or integrity of any part of the work are appropriately investigated and resolved.

Andrea Y. Delgado Medrano was involved in the data acquisition and analysis and has approved the submitted version of the manuscript. She has agreed both to be personally accountable for her contributions and to ensure that questions related to the accuracy or integrity of any part of the work are appropriately investigated and resolved.

Adilene Olvera was involved in the data acquisition and analysis and has approved the submitted version of the manuscript. She has agreed both to be personally accountable for her contributions and to ensure that questions related to the accuracy or integrity of any part of the work are appropriately investigated and resolved.

Jagannadha K. Sastry was involved in the data acquisition and analysis and has approved the submitted version of the manuscript. He has agreed both to be personally accountable for his contributions and to ensure that questions related to the accuracy or integrity of any part of the work are appropriately investigated and resolved.

Patricia J. Eifel was involved in the data acquisition and has approved the submitted version of the manuscript. She has agreed both to be personally accountable for her contributions and to ensure that

questions related to the accuracy or integrity of any part of the work are appropriately investigated and resolved.

Anuja Jhingran was involved in the data acquisition and has approved the submitted version of the manuscript. She has agreed both to be personally accountable for her contributions and to ensure that questions related to the accuracy or integrity of any part of the work are appropriately investigated and resolved.

Lilie L. Lin was involved in the data acquisition and has approved the submitted version of the manuscript. She has agreed both to be personally accountable for her contributions and to ensure that questions related to the accuracy or integrity of any part of the work are appropriately investigated and resolved.

Lois M. Ramondetta was involved in the data acquisition and has approved the submitted version of the manuscript. She has agreed both to be personally accountable for her contributions and to ensure that questions related to the accuracy or integrity of any part of the work are appropriately investigated and resolved.

Andrew M. Futreal was involved in the data acquisition and has approved the submitted version of the manuscript. He has agreed both to be personally accountable for his contributions and to ensure that questions related to the accuracy or integrity of any part of the work are appropriately investigated and resolved.

Amir A. Jazaeri was involved in the data acquisition and has approved the submitted version of the manuscript. He has agreed both to be personally accountable for his contributions and to ensure that questions related to the accuracy or integrity of any part of the work are appropriately investigated and resolved.

Kathleen M. Schmeler was involved in the data acquisition and has approved the submitted version of the manuscript. She has agreed both to be personally accountable for her contributions and to ensure that questions related to the accuracy or integrity of any part of the work are appropriately investigated and resolved.

Jingyan Yue was involved in the data acquisition and analysis and has approved the submitted version of the manuscript. She has agreed both to be personally accountable for her contributions and to ensure that questions related to the accuracy or integrity of any part of the work are appropriately investigated and resolved.

Aparna Mitra was involved in the data acquisition and analysis and has approved the submitted version of the manuscript. She has agreed both to be personally accountable for her contributions and to ensure that questions related to the accuracy or integrity of any part of the work are appropriately investigated and resolved.

Kyoko Yoshida-Court was involved in the data acquisition and analysis and has approved the submitted version of the manuscript. She has agreed both to be personally accountable for her contributions and to ensure that questions related to the accuracy or integrity of any part of the work are appropriately investigated and resolved.

Jennifer Wargo was involved in the data acquisition and has approved the submitted version of the manuscript. She has agreed both to be personally accountable for her contributions and to ensure that questions related to the accuracy or integrity of any part of the work are appropriately investigated and resolved.

Travis Solley was involved in the data acquisition and analysis and has approved the submitted version of the manuscript. He has agreed both to be personally accountable for his contributions and to ensure that questions related to the accuracy or integrity of any part of the work are appropriately investigated and resolved.

Venkatesh Hegde was involved in the data acquisition and analysis and has approved the submitted version of the manuscript. He has agreed both to be personally accountable for his contributions and to ensure that questions related to the accuracy or integrity of any part of the work are appropriately investigated and resolved.

Sita S. Nookala was involved in the data acquisition and analysis and has approved the submitted version of the manuscript. She has agreed both to be personally accountable for her contributions and to ensure that questions related to the accuracy or integrity of any part of the work are appropriately investigated and resolved.

Ananta Yanamandra was involved in the data acquisition and analysis and has approved the submitted version of the manuscript. He has agreed both to be personally accountable for his contributions and to ensure that questions related to the accuracy or integrity of any part of the work are appropriately investigated and resolved.

Stephanie M. Dorta-Estremera was involved in the data acquisition and analysis and has approved the submitted version of the manuscript. She has agreed both to be personally accountable for her contributions and to ensure that questions related to the accuracy or integrity of any part of the work are appropriately investigated and resolved.

Geena G. Mathew was involved in the data acquisition and has approved the submitted version of the manuscript. She has agreed both to be personally accountable for her contributions and to ensure that questions related to the accuracy or integrity of any part of the work are appropriately investigated and resolved.

Rohit Kavukuntla was involved in the data acquisition and has approved the submitted version of the manuscript. He has agreed both to be personally accountable for his contributions and to ensure that

questions related to the accuracy or integrity of any part of the work are appropriately investigated and resolved.

Cassidy Papso was involved in the data acquisition and has approved the submitted version of the manuscript. She has agreed both to be personally accountable for her contributions and to ensure that questions related to the accuracy or integrity of any part of the work are appropriately investigated and resolved.

Mustapha Ahmed-Kaddar was involved in the data acquisition and analysis and has approved the submitted version of the manuscript. He has agreed both to be personally accountable for his contributions and to ensure that questions related to the accuracy or integrity of any part of the work are appropriately investigated and resolved.

Minsoo Kim was involved in the data acquisition and analysis and has approved the submitted version of the manuscript. He has agreed both to be personally accountable for his contributions and to ensure that questions related to the accuracy or integrity of any part of the work are appropriately investigated and resolved.

Jianhua Zhang was involved in the data acquisition and analysis and has approved the submitted version of the manuscript. He has agreed both to be personally accountable for his contributions and to ensure that questions related to the accuracy or integrity of any part of the work are appropriately investigated and resolved.

Alexandre Reuben was involved in the data acquisition and analysis and has approved the submitted version of the manuscript. He has agreed both to be personally accountable for his contributions and to ensure that questions related to the accuracy or integrity of any part of the work are appropriately investigated and resolved.

Emma B. Holliday was involved in the data acquisition and has approved the submitted version of the manuscript. She has agreed both to be personally accountable for her contributions and to ensure that questions related to the accuracy or integrity of any part of the work are appropriately investigated and resolved.

Bruce D. Minsky was involved in the data acquisition and has approved the submitted version of the manuscript. He has agreed both to be personally accountable for his contributions and to ensure that questions related to the accuracy or integrity of any part of the work are appropriately investigated and resolved.

Albert Koong was involved in the data acquisition and has approved the submitted version of the manuscript. He has agreed both to be personally accountable for his contributions and to ensure that questions related to the accuracy or integrity of any part of the work are appropriately investigated and resolved.

Eugene J. Koay was involved in the data acquisition and has approved the submitted version of the manuscript. He has agreed both to be personally accountable for his contributions and to ensure that questions related to the accuracy or integrity of any part of the work are appropriately investigated and resolved.

Prajnan Das was involved in the data acquisition and has approved the submitted version of the manuscript. He has agreed both to be personally accountable for his contributions and to ensure that questions related to the accuracy or integrity of any part of the work are appropriately investigated and resolved.

Cullen M. Taniguchi was involved in the data acquisition and has approved the submitted version of the manuscript. He has agreed both to be personally accountable for his contributions and to ensure that questions related to the accuracy or integrity of any part of the work are appropriately investigated and resolved.

Ann H. Klopp was involved in the study design, data acquisition, analysis and interpretation, and has drafted and approved the submitted version of the manuscript. She has agreed both to be personally accountable for her contributions and to ensure that questions related to the accuracy or integrity of any part of the work are appropriately investigated and resolved.

Competing Interests

ACK holds stock in Aravive, Inc., and also serves as a consultant. PD reports personal fees from Adlai Nortye, personal fees from MD Anderson Cancer Center Madrid Spain, outside the submitted work.

References

1. Formenti, S. C. & Demaria, S. Radiation Therapy to Convert the Tumor Into an In Situ Vaccine. *Int. J. Radiat. Oncol.* **84**, 879–880 (2012).
2. Antonia, S. J. *et al.* Durvalumab after Chemoradiotherapy in Stage III Non-Small-Cell Lung Cancer. *N. Engl. J. Med.* **377**, 1919–1929 (2017).
3. Grimaldi, A. M. *et al.* Abscopal effects of radiotherapy on advanced melanoma patients who progressed after ipilimumab immunotherapy. *Oncoimmunology* **3**, e28780 (2014).
4. Reits, E. A. *et al.* Radiation modulates the peptide repertoire, enhances MHC class I expression, and induces successful antitumor immunotherapy. *J. Exp. Med.* **203**, 1259–1271 (2006).
5. Demaria, S. & Formenti, S. C. Role of T lymphocytes in tumor response to radiotherapy. *Front. Oncol.* **2**, 95 (2012).
6. Lhuillier, C., Rudqvist, N.-P., Elemento, O., Formenti, S. C. & Demaria, S. Radiation therapy and anti-tumor immunity: exposing immunogenic mutations to the immune system. *Genome Med.* **11**, 40 (2019).
7. Hausen, H. zur. Viruses in Human Cancers. *Science* **254**, 1167–1173 (1991).

8. Borysiewicz, L. K. *et al.* A recombinant vaccinia virus encoding human papillomavirus types 16 and 18, E6 and E7 proteins as immunotherapy for cervical cancer. *The Lancet* **347**, 1523–1527 (1996).
9. da Costa, S. C. S. *et al.* Neoadjuvant Chemotherapy With Cisplatin and Gemcitabine Followed by Chemoradiation Versus Chemoradiation for Locally Advanced Cervical Cancer: A Randomized Phase II Trial. *J. Clin. Oncol. Off. J. Am. Soc. Clin. Oncol.* **37**, 3124–3131 (2019).
10. Liu, C., Mann, D., Sinha, U. K. & Kokot, N. C. The molecular mechanisms of increased radiosensitivity of HPV-positive oropharyngeal squamous cell carcinoma (OPSCC): an extensive review. *J. Otolaryngol. - Head Neck Surg.* **47**, (2018).
11. Massarelli, E. *et al.* Combining Immune Checkpoint Blockade and Tumor-Specific Vaccine for Patients With Incurable Human Papillomavirus 16–Related Cancer: A Phase 2 Clinical Trial. *JAMA Oncol.* **5**, 67–73 (2019).
12. Melief, C. J. M. *et al.* Strong vaccine responses during chemotherapy are associated with prolonged cancer survival. *Sci. Transl. Med.* **12**, (2020).
13. Welters, M. J. *et al.* Vaccination during myeloid cell depletion by cancer chemotherapy fosters robust T cell responses. *Sci. Transl. Med.* **8**, 334ra52-334ra52 (2016).
14. Poelgeest, M. I. E. van *et al.* Vaccination against Oncoproteins of HPV16 for Noninvasive Vulvar/Vaginal Lesions: Lesion Clearance Is Related to the Strength of the T-Cell Response. *Clin. Cancer Res.* **22**, 2342–2350 (2016).
15. Sluis, T. C. van der *et al.* Vaccine-Induced Tumor Necrosis Factor–Producing T Cells Synergize with Cisplatin to Promote Tumor Cell Death. *Clin. Cancer Res.* **21**, 781–794 (2015).
16. Kenter, G. G. *et al.* Vaccination against HPV-16 Oncoproteins for Vulvar Intraepithelial Neoplasia. *N. Engl. J. Med.* **361**, 1838–1847 (2009).
17. Del Mistro, A. *et al.* Human papilloma virus genotyping for the cross-sectional and longitudinal probability of developing cervical intraepithelial neoplasia grade 2 or more. *Int. J. Cancer* **143**, 333–342 (2018).
18. Wang, X., Zeng, Y., Huang, X. & Zhang, Y. Prevalence and Genotype Distribution of Human Papillomavirus in Invasive Cervical Cancer, Cervical Intraepithelial Neoplasia, and Asymptomatic Women in Southeast China. *BioMed Res. Int.* **2018**, 2897937 (2018).
19. Isidean, S. D. *et al.* Human papillomavirus testing versus cytology in primary cervical cancer screening: End-of-study and extended follow-up results from the Canadian cervical cancer screening trial. *Int. J. Cancer* **139**, 2456–2466 (2016).
20. Glanville, J. *et al.* Identifying specificity groups in the T cell receptor repertoire. *Nature* **547**, 94–98 (2017).
21. Tickotsky, N., Sagiv, T., Prilusky, J., Shifrut, E. & Friedman, N. McPAS-TCR: a manually curated catalogue of pathology-associated T cell receptor sequences. *Bioinformatics* **33**, 2924–2929 (2017).
22. Münger, K., Phelps, W. C., Bubb, V., Howley, P. M. & Schlegel, R. The E6 and E7 genes of the human papillomavirus type 16 together are necessary and sufficient for transformation of primary human keratinocytes. *J. Virol.* **63**, 4417–4421 (1989).

23. Scrucca, L., Fop, M., Murphy, T. B. & Raftery, A. E. mclust 5: Clustering, Classification and Density Estimation Using Gaussian Finite Mixture Models. *R J.* **8**, 289–317 (2016).
24. Cui, J.-H. *et al.* TCR Repertoire as a Novel Indicator for Immune Monitoring and Prognosis Assessment of Patients With Cervical Cancer. *Front. Immunol.* **9**, (2018).
25. Danilova, L. *et al.* The Mutation-Associated Neoantigen Functional Expansion of Specific T Cells (MANAFEST) Assay: A Sensitive Platform for Monitoring Antitumor Immunity. *Cancer Immunol. Res.* **6**, 888–899 (2018).
26. Dorta-Estremera, S. *et al.* Kinetics of Intratumoral Immune Cell Activation During Chemoradiation for Cervical Cancer. *Int. J. Radiat. Oncol.* **102**, 593–600 (2018).
27. Shugay, M. *et al.* VDJdb: a curated database of T-cell receptor sequences with known antigen specificity. *Nucleic Acids Res.* **46**, D419–D427 (2018).
28. Zhang, W. *et al.* PIRD: Pan Immune Repertoire Database. *Bioinformatics* **36**, 897–903 (2020).
29. Nazarov, V., Immunarch.Bot & Rumynskiy, E. *immunomind/immunarch: 0.6.5: Basic single-cell support*. (Zenodo, 2020). doi:10.5281/ZENODO.3893991.
30. RStudio Team. *RStudio: Integrated Development for R.* (RStudio, Inc., 2020).

Table

Table 1. Patient demographic and clinical characteristics (n=86)

	N	%
Age, years, Mean (SD)	49.07 (11.5)	—
BMI, kg/m^2, Mean (SD)	29.41 (6.57)	—
Type of Cancer		
Cervical	67	77.9
Anal	14	16.3
Vaginal	4	4.6
Vulvar	1	1.2
Histology		
Squamous cell carcinoma	73	84.9
Adenocarcinoma	10	11.6
Adenosquamous carcinoma	3	3.5
Node Status		
Positive	60	69.8
Negative	26	30.2
Stage		
I	17	19.8
II	33	38.4
III	29	33.7
IV	7	8.1
HPV Status		
Positive	52	60.5
Negative	8	9.3
Not tested	26	30.2
HPV Strain (n=38)		
HPV 16	23	60.5
HPV 18	8	21.1
HPV 58	4	10.5
HPV 33	3	7.9
HPV 35	3	7.9
HPV 52	3	7.9
HPV 72	3	7.9
HPV 61	2	5.3
HPV 62	2	5.3
HPV 39	2	5.3
HPV 45	2	5.3
HPV 71	2	5.3
HPV 39	1	2.3
HPV 31	1	2.3
HPV 73	1	2.3
HLA Type (N=7)		
A01	1	—
A02	4	—
A02:01	1	—
A02:33	1	—
A03	2	—
A26	1	—
A31	2	—
A32	1	—
A36	1	—
B07	2	—
B15	2	—

B18	1	—
B37	2	—
B37:01	1	—
B38	1	—
B39:06	1	—
B44	1	—
B47:01	1	—
B50:01	1	—
B53	1	—
C03	2	—
C04	2	—
C05	2	—
C06	2	—
C06:02	2	—
C07	3	—
C12	1	—

Figures

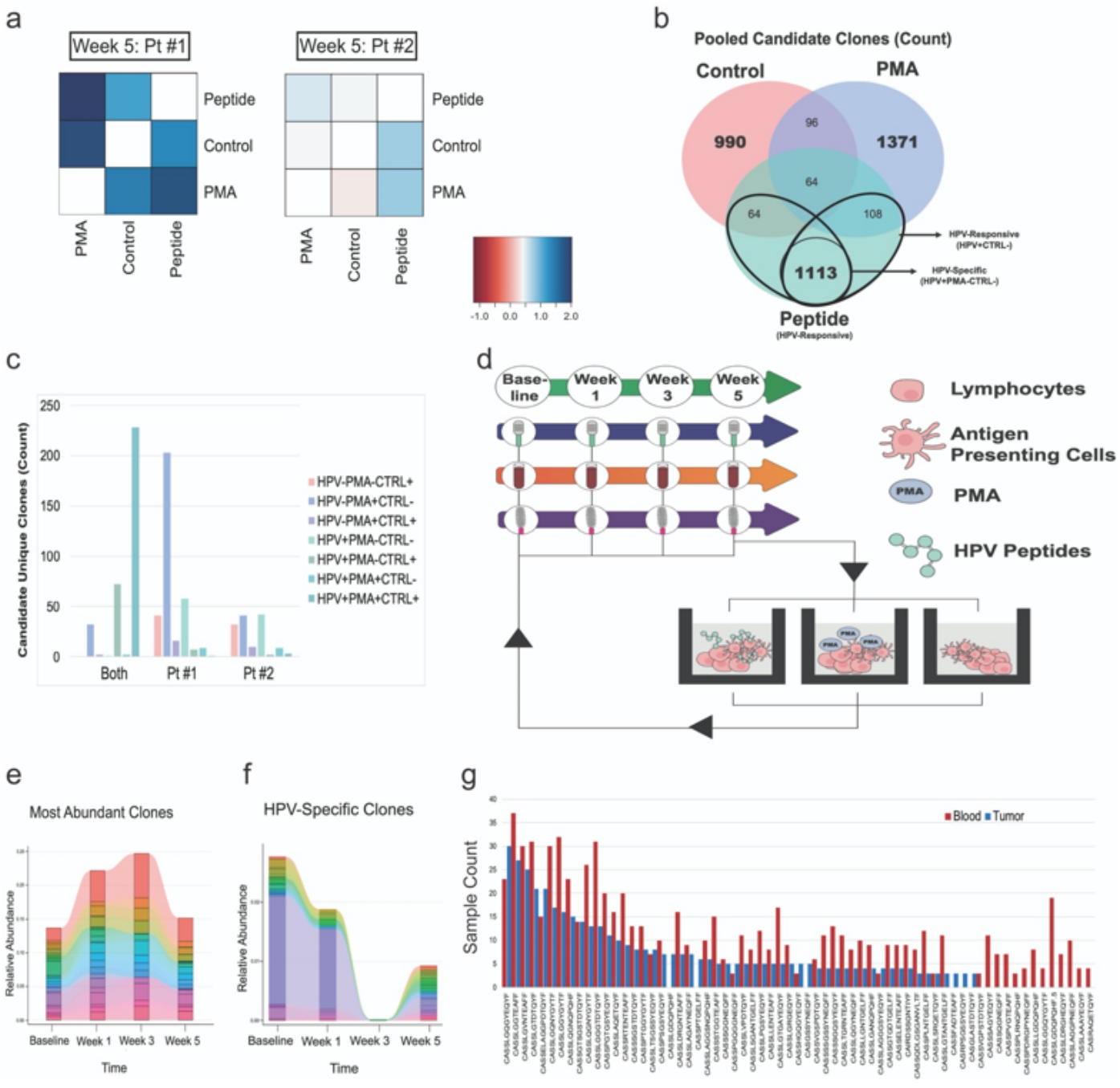

Figure 1

HPV-specific clones in HPV-related cancers in patients undergoing CRT. a. Morisita overlap indices for 2 patients using pools on the x-axis as the reference. b. Description of pooled candidate clones from both patients. A Venn diagram shows the 7 categories and numbers of clones included in each. c. Clones of each category present in both patients (Both), in only patient #1 (Pt #1), or in only patient #2 (Pt #2). d. Tumor swabs, peripheral blood, and tumor cytobrushes were collected from each patient before (baseline) and during (week 1, week 3, week 5) chemoradiation therapy. DNA was isolated from one subset of blood and tumor samples, and the other subset was analyzed by flow cytometry. T cell receptor sequencing was performed on isolated tumor and blood DNA, and the results were analyzed for the

presence of HPV-specific and HPV-responsive clones identified through an antigen-stimulation assay performed on 2 patients' tumor cells at week 5. Cells collected from tumor cytobrushes were incubated overnight in 3 wells containing an HPV peptide cocktail, a PMA cocktail, or only media. TCR sequencing was performed on DNA isolated from cells from each of these wells, and HPV-specific and HPV-responsive clones were identified as shown in (c). The TCR sequencing results for the study population were analyzed with regard to these HPV-specific and HPV-responsive clones. e,f. Relative abundance of HPV-specific clones (e) and most abundant clones (f) at baseline, week 1, week 3, and week 5. g. Numbers of samples within the study population with HPV-specific clones present in blood (red) and tumor (blue).

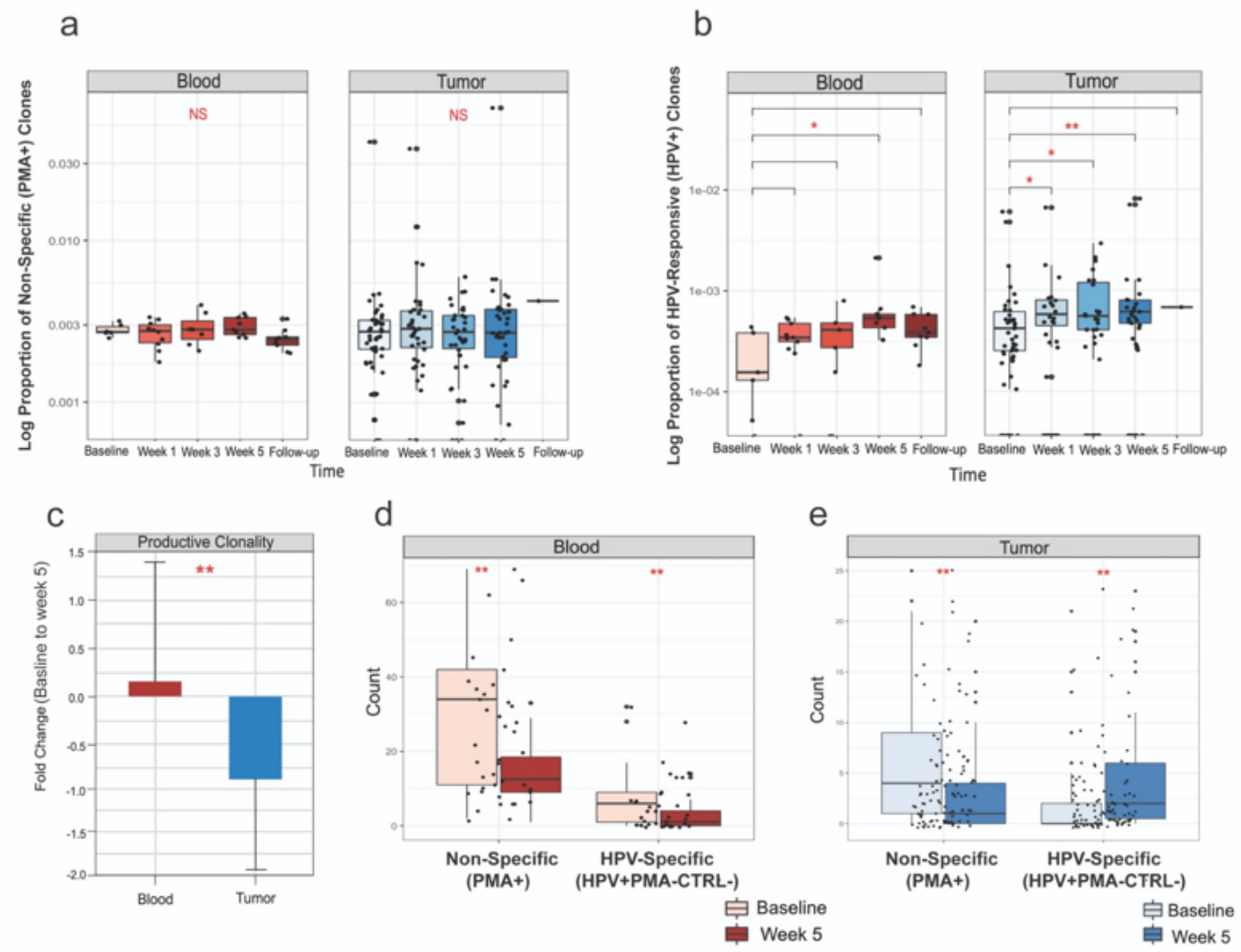

Figure 2

HPV-responsive T-cell remodeling differs from overall T-cell remodeling. a. Log proportion of non-specific (PMA+) clones before, during, and after chemoradiation therapy in both blood (left) and tumor (right). Significant changes between each time point and baseline were determined using the Wilcoxon signed-rank test. b. Log proportion of HPV-responsive (HPV+) clones before, during and after CRT in both blood

(left) and tumor (right). Significant changes between each time point and baseline were determined using the Wilcoxon signed-rank test. c. Productive clonality fold-change from baseline to week 12 in blood and tumor. Paired Wilcoxon signed-rank tests were performed. Bars represent standard errors. d. Absolute count of non-specific (PMA+) and HPV-specific (HPV+PMA-CTRL-) clones in blood at baseline and at week 5. Paired Wilcoxon signed-rank tests were performed. e. Absolute count of non-specific (PMA+) and HPV-specific (HPV+PMA-CTRL-) clones in tumor at baseline and at week 5. Paired Wilcoxon signed-rank tests were performed. For blood: baseline n = 18, week 1 n = 21, week 3 n = 18, week 5 n = 18, week 12 n = 12. For tumor: baseline n = 61, week 1 n = 53, week 3 n = 51, week 5 n = 51, week 12 n = 6. The thick middle line of each boxplot represents the median, and the lower and upper bounds of the box represent the first and third quartiles, respectively. Whiskers extend 1.5 times the interquartile range below the first quartile and above the third quartile. NS = not significant, *P < 0.05, **P < 0.01.

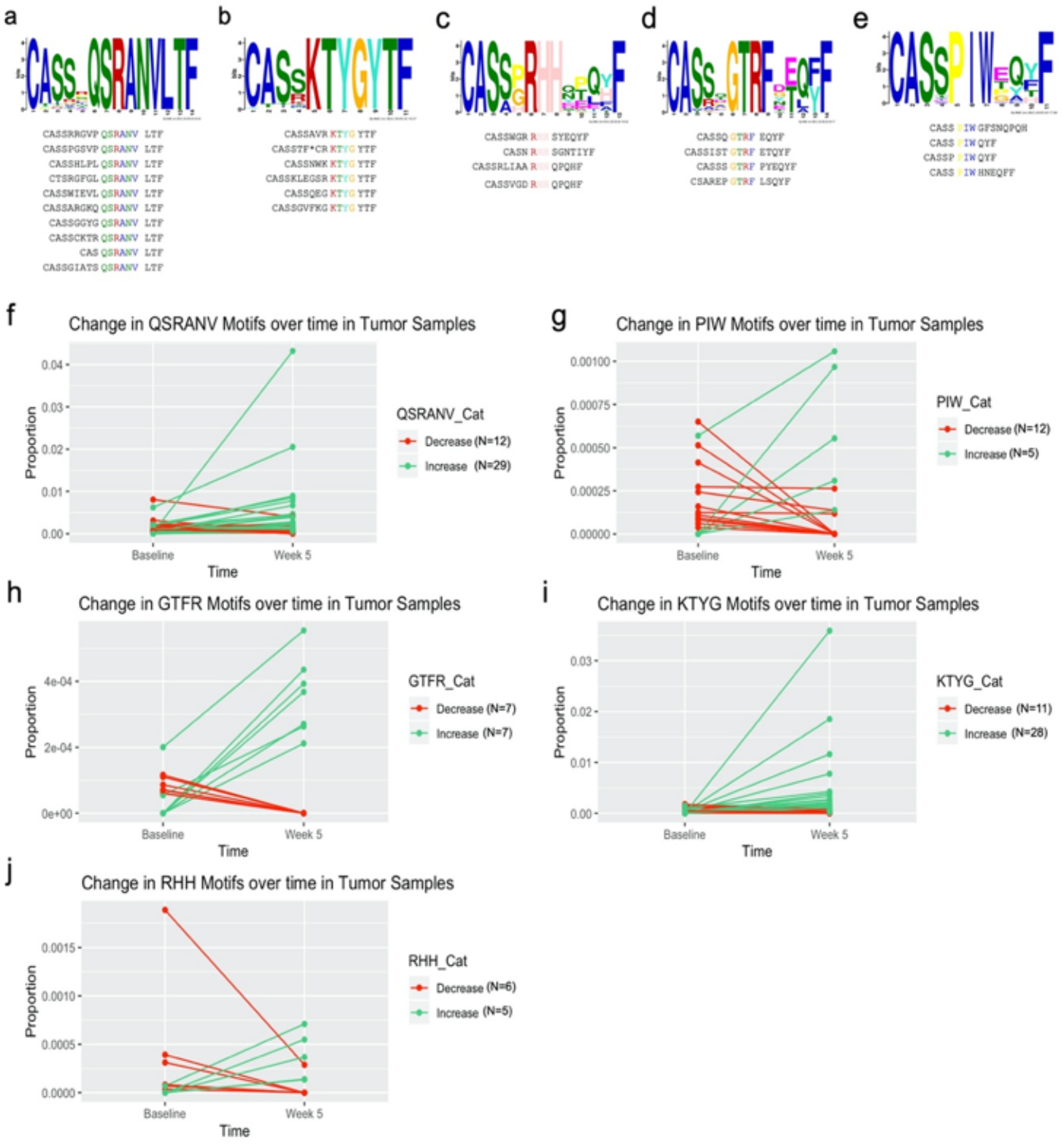

Figure 3

TCR motifs are enriched in HPV-reactive T-cell populations. a-e. Five TCR amino acid motifs were identified in HPV peptide-stimulated T-cell populations using the GLIPH (Grouping of Lymphocyte Interactions by Paratope Hotspots) clustering algorithm. Representations of the CDR3β receptor amino acid alignment for each of the motifs identified in HPV-stimulated T-cell populations are shown: QSRANV (a), KTYG (b), PIW (c), RHH (d), and GTRF (e). Motifs were cross-referenced with TCR sequences

recovered from all patients. The corresponding sequence logo shown in the top panel illustrates the amino acid sequence conservation across TCRs recovered from all patients containing each motif. Sequence logos were generated using the GLAM2 software tool.26 The size of each letter corresponds with its degree of conservation in the amino acid sequence. f-j. Individual motifs are plotted for all patients. Each plot shows the changes in the proportions of the QSRANV (f), PIW (g), GTFR (h), KTYG (i), and RHH (j) motifs in tumor samples between baseline and week 5. Each line denotes an individual patient. Most patients experienced an increase in motif proportion by week 5. Green lines represent increases in motif proportion from baseline to week 5, and red lines represent decreases. Patients who did not have motifs at either time point were excluded from the line plots.

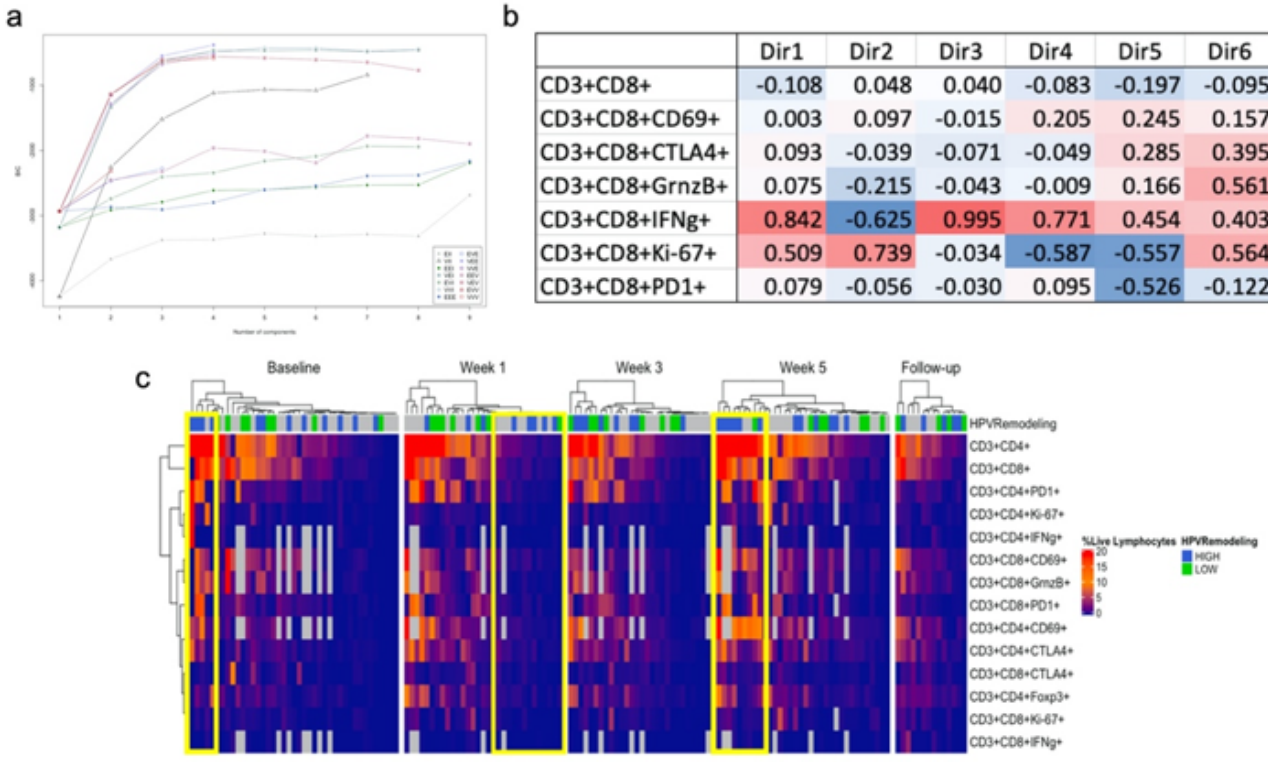

	Dir1	Dir2	Dir3	Dir4	Dir5	Dir6	Dir7
CD3+CD8+	-0.108	0.048	0.040	-0.083	-0.197	-0.095	0.058
CD3+CD8+CD69+	0.003	0.097	-0.015	0.205	0.245	0.157	-0.080
CD3+CD8+CTLA4+	0.093	-0.039	-0.071	-0.049	0.285	0.395	0.591
CD3+CD8+GrnzB+	0.075	-0.215	-0.043	-0.009	0.166	0.561	-0.129
CD3+CD8+IFNg+	0.842	-0.625	0.995	0.771	0.454	0.403	0.402
CD3+CD8+Ki-67+	0.509	0.739	-0.034	-0.587	-0.557	0.564	-0.681
CD3+CD8+PD1+	0.079	-0.056	-0.030	0.095	-0.526	-0.122	0.005

Figure 4

Immune cluster phenotypes associated with HPV remodeling during CRT a. The Bayesian information criterion for parameterized Gaussian mixture models fitted by the expectation-maximization algorithm initialized by model-based hierarchical clustering using mclust. b. Estimated basis vectors for CD3+CD8+ cells in tumor samples (in response to peptide) using predicted model boundaries from mclust. C. Unsupervised clustering of CD4+ and CD8+ markers labelled by HPV remodeling status.

Supplementary Files

This is a list of supplementary files associated with this preprint. Click to download.

- SupplementalFigures.docx

- SupplementalTable1.xlsx
- SupplementalTable2.csv
- SupplementalTable3.csv
- SupplementalTable4.xlsx
- SupplementalTable5.xlsx
- SupplementalTable6.pdf
- SupplementalTable7.xlsx
- SupplementalTable8.xlsx
- SupplementalTable9.xlsx
- SupplementalTable10.pdf
- SupplementalTable11.pdf